Dual-Polarized Microstrip Patch Antenna Array with Dual-Feed for Target Detection

Ki-Baek Kim
The Affiliated Institute of Electronics Telecommunications Research Instituute
Daejeon, Republic of Korea
kbkim11@nsr.re.kr

Bang Chul Jung
The Department of Electronics Engineering
Chungnam National University
Daejeon, Republic of Korea
bcjung@cnu.ac.kr

Jong-Myung Woo
The department of Radio and Information Communications Engineering
Chungnam National University
Daejeon, Republic of Korea
jmwoo@cnu.ac.kr

***Abstract*—A planar antenna is designed to replace complex structures of many rat-race couplers and 90° hybrids used in conventional target detection antennas. The proposed antenna has 2 x 2 microstrip patch antenna arrays with dual feeding to radiate symmetric polarizations in the 9.375 GHz (X-band). The sum pattern with circular polarization is implemented through a sequence feeding at port 1. The simultaneous feeding of port 2 radiates a difference pattern in all polarizations. Thus, a target detection antenna is designed with features that have fewer ports than the conventional monopulse antennas. The proposed antenna is compact, planar, and has a simple comparator circuit and equal sum and difference levels. Also, in the last section, the antenna feeding network which can be receive the dual-CP (RHCP and LHCP) is proposed.**

Keywords— Microstrip patch array, target detection antenna, dual feed microstrip patch

I. Introduction

Monopulse antennas are used for direction finding (DF) and communication signal tracking of radar and satellite systems by using sum (Σ) and difference (Δ) patterns [1].

In the conventional DF, monopulse antennas use a cassegrain parabolic and a lens antenna. These antennas and monopulse comparators are very complex, heavy, and require high production costs. In contrast, a microstrip structure can significantly reduce the cost of fabrication and weight, which is printed on the substrate. Various monopulse antennas and comparators using the microstrip structure have been developed for the DF [2-13]. In [1], the structure with helix antenna array and three rat-race coupler (180° hybrid) was proposed.

In [2], the structure with helix antenna array and three rat-race couplers (180° hybrid) was proposed. In [3], the monopulse comparator with four 180° hybrids was proposed. In [4]-[6], the structure with three quadrature hybrids (90° hybrid) and a phase delay line was proposed. In [7]-[10], the structure with substrate integrated waveguide (SIW) was proposed. However, the structures proposed in [2]-[10] have complex circuits such as rat-race coupler and require at least 3 or 4 ports for monopulse applications. As a results those structures induce the large size and high cost for implementation.

On the other hand, a less complex antenna with two ports was proposed in [11], but the difference (Δ) pattern has only one polarization. A broadband monopulse antenna using the conical 4-arm spiral was proposed in [12], [13], but it requires to switch to radiate the sum (Σ) or difference (Δ) pattern. Thus, the antennas in [12], [13] are large and cannot radiate both the patterns simultaneously.

In this paper, we propose a compact type of antenna with two ports for precise target detection, thereby replacing the complex comparator circuits. The designed antenna is printed on a substrate for low-profile and easy fabrication. The first port synthesizes a sum (Σ) pattern with circular polarization (LHCP and RHCP) by the sequence feeding of four microstrip patch antennas. The other port has new symmetrical feeding positions of antennas to make a difference (Δ) pattern for the all polarizations. The simulated and measured results for the designed antenna are presented. Also, in the last section, the antenna feeding network is proposed to receive both RHCP and LHCP.

II. Antenna Design

Fig. 1 shows the structure of the designed antenna. The detailed dimensions are shown in Table 1. Teflon (ε_r = 2.5) is used as the substrate and its size is 80 (4λ) mm x 80 (4λ) mm (where λ = wavelength of 9.375 GHz). The substrate has two printed sides of microstrip patch antennas (thickness, t1 = 1.6 mm) and feeding line (thickness, t2 = 0.8 mm).

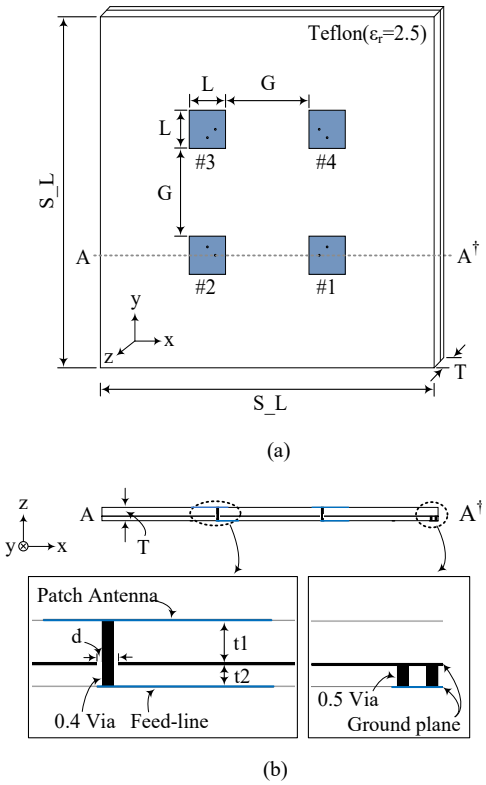

Fig. 1. Structure of the designed antenna. (a) Top view. (b) Cutting plane of A-A†.

978-83-949421-7-5 ©2020 Warsaw University of Technology

TABLE I. DIMENSIONS OF THE DESIGNED ANTENNA

Parameters	Symbol	Value (mm)
Length of the substrate	S_L	80 (4λ)
Gap of patch antennas	G	20 (1λ)
Length of patch antennas	L	8.7
Diameter of via hole	d	0.6
Thickness of the proposed antenna	T	2.4
Thickness of the antenna substrate	t1	1.6
Thickness of the feeding line substrate	t2	0.8
Width of 70 Ω line	w1	1.21
Width of 100 Ω line	w2	0.58

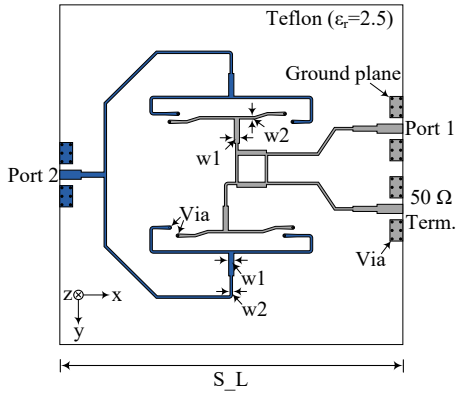

Fig. 2. The bottom view of the designed antenna.

As shown in Fig. 1(a), the 2 x 2 microstrip patch antenna array, was designed in a square structure with a length (L) of 8.7 mm to match 9.375 GHz (X-band). The gap (G) between the patch antennas shall be selected by considering the equal level of sum (Σ) and difference (Δ) and the placement of T-junction power divider and 90° hybrid on the backside.

Fig. 1(b) shows a cross section (A to A†) on Fig. 1(a). The antenna patch is connected to the feed line through a 0.4 mm diameter via. A hole (d) of 0.6 mm diameter is made on the center of the ground plane to separate the vias from the ground electrically. To the right, the ground plane was extended using a 0.5 mm diameter via to connect the SMA connector of the port on the backside.

Fig. 2 shows the feeding lines on the backside. The two input ports are 50 Ω lines, and the impedance of the line to the antenna through the T-junction power divider and 90° hybrid is 100 Ω (0.58 mm). Port 1 is used by 90° hybrid and 90° phase delay line in the center of the antenna to provide 180°. Port 2 uses three T-junction power dividers to generate a difference (Δ) pattern, with an in-phase feed to the four microstrip patch antennas.

As shown in Fig. 3(a), the phase difference between point A and point B over the 90° hybrid and phase delay (90°) line is 180°, with the phase difference of position C-D and E-F. Thus, the four microstrip patch antennas are designed to have sequential feeding (C-point 0°, D-point 90°, E-point 180°, F-point 270°). As shown in Fig. 3(b), port 1 generates a sum (Σ) pattern with LHCP. Conversely, in Fig. 3(c), the four microstrip patch antennas are designed to have sequential feeding (D-point 0°, C-point 90°, F-point 180°, E-point 270°).

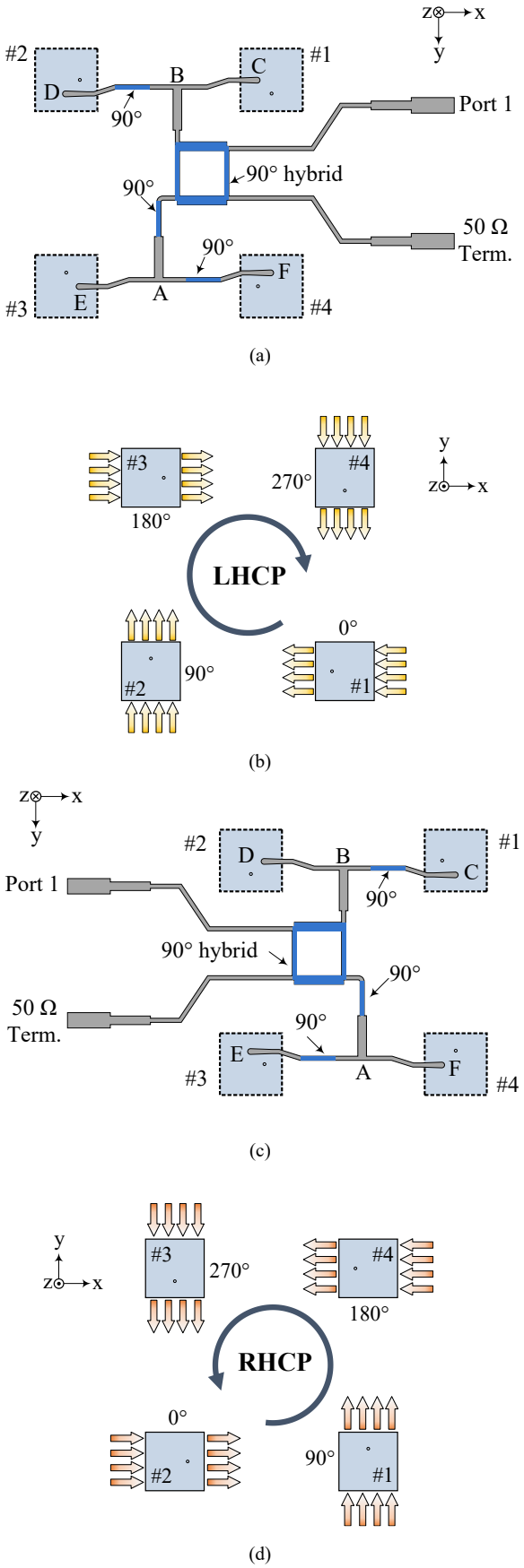

Fig. 3. Feeding network of the port 1. (a) The sequential feeding for LHCP. (b) LHCP radiation of the micrrostrip patch array. (c) The sequential feeding for RHCP. (d) RHCP radiation of the micrrostrip patch array.

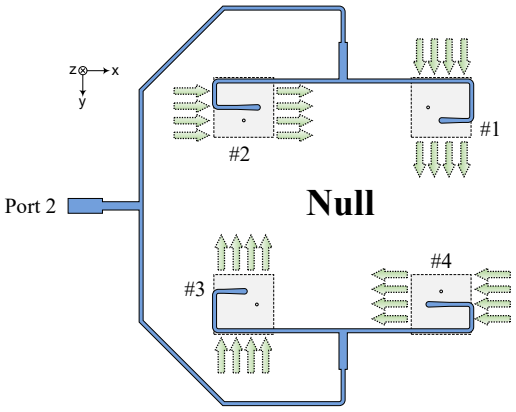

Fig. 4 Feeding network of the port 2

TABLE II. THE HPBW, GAIN AND SLL OF THE SUM PATTERN

G (mm)	HPBW (deg.)	Gain (dBi)	SLL (dB)
10	48.8	6.57	-10.4
12	44.8	6.95	-9.1
14	41	7.09	-7.8
16	37.2	7.12	-6.5
18	33.7	7.06	-5.6
20	30.5	6.97	-4.8
22	27.7	6.95	-4.3
24	25.6	6.90	-4.0
26	23.9	6,91	-3.8
28	22.5	6.93	-3.7
30	21.1	7.03	-3.8

As shown in Fig. 3(d), port 1 generates a sum (Σ) pattern with RHCP.

Therefore, the proposed antenna can be freely designed to have LHCP or RHCP, depending on the configuration of the feeding network of port 1. In this paper, the feeding network of port 1 is fabricated with LHCP as shown in Fig. 3(a).

Port 2 simultaneously feeds to the antenna through T-junction power divider as Fig. 4. Feed lines are placed in a symmetrical structure to deliver the same phase to all the four antennas. The symmetrical feeding positions of the microstrip patch antenna provide different polarizations from a single antenna. The polarizations cancel each other and create a null point in the center of the antenna.

The side lobe levels (SLL), maximum gain and half power beam widths (HPBW) of sum (Σ) patterns are shown in Table 2. The radiation patterns of the sum (Σ) and difference (Δ) with different the gap (5 mm ~ 30 mm) are simulated and shown in Fig. 5. At low G, the difference (Δ) patterns are distorted. Higher G leads to increase gain and directivity, the side lobe level (SLL) increase and half power beam width (HPBW) of sum patterns decrease. Therefore, the gap (G) between the patch antennas is 20 mm considering optimum HPBW, peak gain, and SLL.

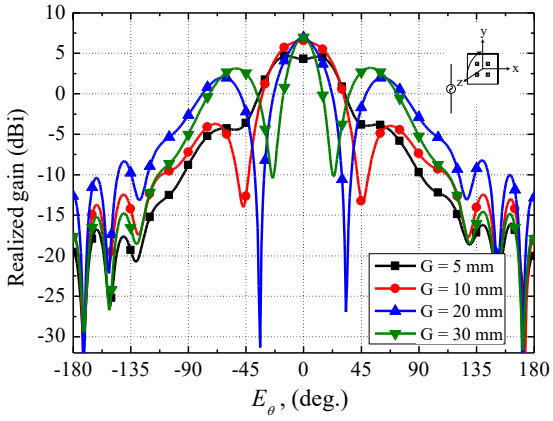

(a)

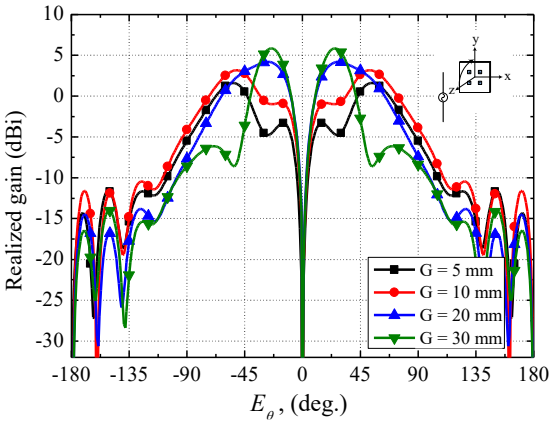

(b)

Fig. 5. The radiation patterns with gap (G) at 9.375 GHz. (a) The sum (Σ) pattern in yz-plane. (b) The difference (Δ) pattern in yz-plane.

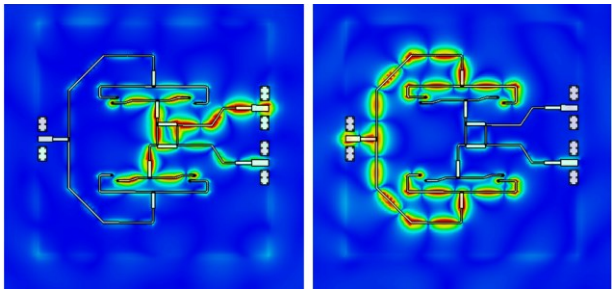

(a) (b)

Fig. 6. *E*-field distribution of the feeding network at 9.375 GHz. (a) Sequential feeding of port 1. (b) Simultaneously feeding of port 2 (in-phase).

Fig. 6 shows the electric field distribution of the feeding network. In Fig. 6(a), the signals that are excited to port 1 are sequentially transmitted through the 90° hybrid and phase delay (90°) lines. Port 2 in Fig. 6(b) transmit a signal with in-phase to each microstrip patch antenna through the T-junction power dividers.

Thus, the designed antenna can detect the direction of the movement of the target using the difference between the sum (Σ) and difference (Δ) patterns during detection signal processing.

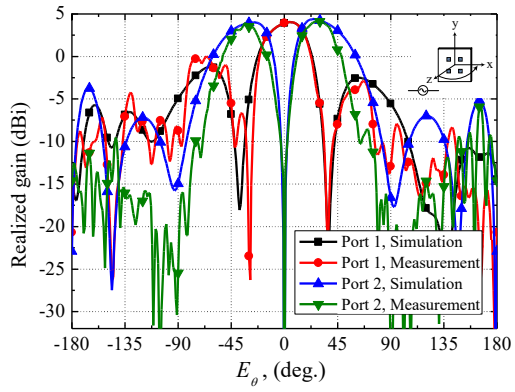

(a)

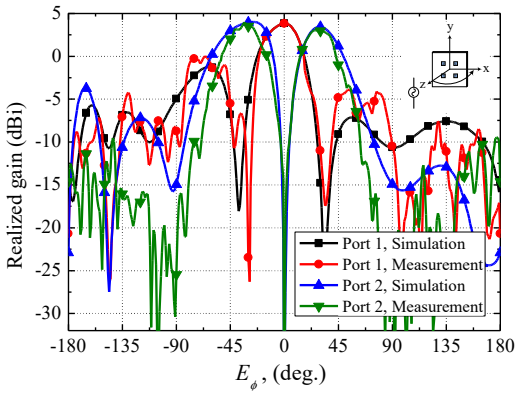

(b)

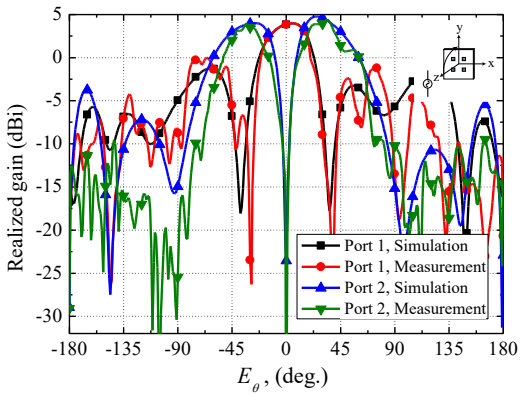

(c)

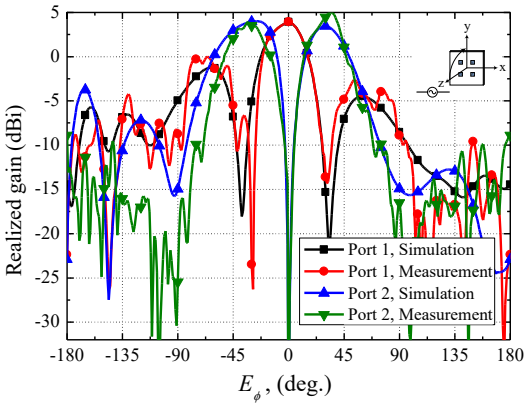

(d)

Fig. 7. Radiation patterns of proposed antenna. (a) E_θ in xz-plane. (b) E_ϕ in xz-plane. (c) E_θ in yz-plane. (d) E_ϕ in yz-plane.

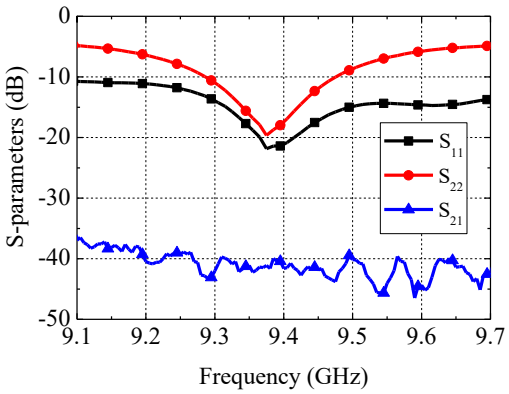

Fig. 8. Measured S-parameters

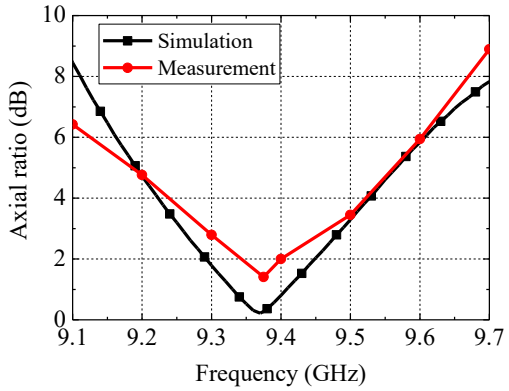

Fig. 9. The axial ratio of the port 1

To enhance detection capability, the difference (Δ) pattern level is designed to be the same as the sum (Σ) pattern level. A sequential comparison of the difference in level between the sum (Σ) and the difference (Δ) patterns can make directional detection more effective.

III. Simulated and Measured Results

Fig. 7 shows a comparison of the simulated and measured radiated patterns at 9.375 GHz. A simulation is performed using CST Microwave Studio 2019. Radiation patterns were measured in an anechoic chamber under far field conditions. Good agreement is observed between the simulation and measurement. In Fig. 7(a) and Fig. 7(b), the radiation pattern of sum (Σ) in xz-plane is shown. Fig. 7(c) and Fig. 7(d) show plotting of the radiation patterns in yz-plane.

The peak gain for the sum (Σ) pattern was measured 3.73 dBi ~ 3.91 dBi, and difference (Δ) pattern was measured 4.30 dBi ~ 4.51 dBi. The difference (Δ) pattern is formed uniformly for all polarization. The proposed antenna has the same peak level of sum (Σ) and difference (Δ) pattern. The measured null depth is less than –34.5 dB and HPBW are 22.5° ~ 40° of sum (Σ) pattern in both azimuth and elevation planes.

Fig. 8 shows the results of measured the S-parameters (S_{11}, S_{22}, and S_{21}) of port 1 and 2. –10 dB bandwidth is 185 MHz (9.29 GHz ~ 9.475 GHz) and isolation of two ports is –41.1 dB at 9.375 GHz. Fig. 9 shows the axial ratio of the sum (Σ) pattern with the simulation results. The measured 3 dB bandwidth of the axial ratio is 160 MHz (9.29 GHz ~ 9.45 GHz).

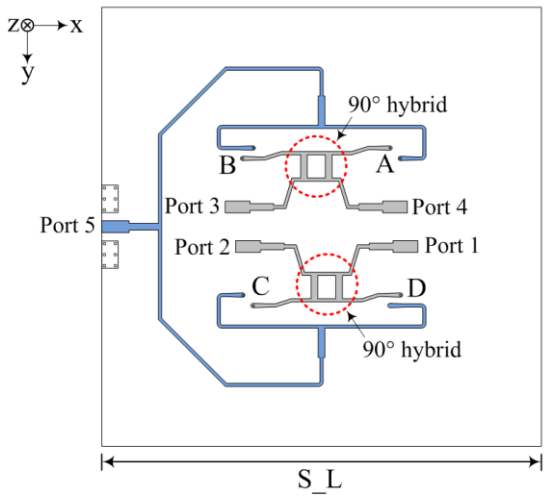

(a)

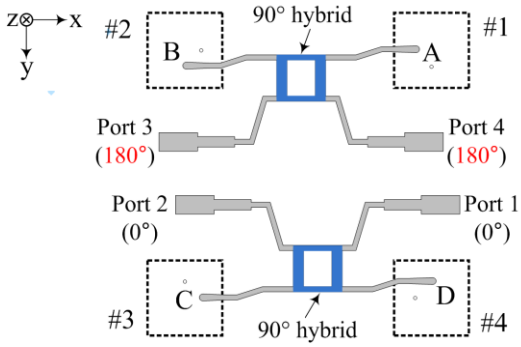

(b)

Fig. 10. Structure of the dual-CP antenna. (a) The bottom view of dual-CP antenna. (b) Antenna feeding network for CP.

IV. Dual-CP Antenna Design

The target detection antenna introduced in the previous section can receive only one type of circular polarization (RHCP or LHCP). The target detection antenna with the LHCP feeding circuit (Fig. 3(a)) cannot receive RHCP. Conversely, the target detection antenna with the RHCP signals feeding circuit (Fig. 3(c)) also cannot receive LHCP signals. To improve this performance, a dual-CP (circular polarization) antenna that can receive both LHCP and RHCP is proposed in this section.

Fig. 10(a) shows the feeding lines on the backside of dual-CP antenna. A substrate of the same size (80 mm x 80 mm) and thickness (0.8 mm) as shown in Fig. 2 is used. The feeding network is connected to a 2 x 2 microstrip patch antenna array the same as the target detection antenna. From port 1 to port 4 generate the sum (Σ) patterns (CP) through sequential feeding and the port 5 generates the difference (Δ) patterns.

Fig. 10(b) shows the feeding network for the sum (Σ) patterns. To generate RHCP, port 1 with 0° and port 3 with 180° phase delay are fed simultaneously through the power divider. Through the 90° hybrid, the point A and B, C and D have 90° phase difference, respectively. Thus, the four microstrip patch antennas have sequential feeding (D-point 0°, C-point 90°, B-point 180°, A-point 270°) and generate the RHCP sum (Σ) pattern.

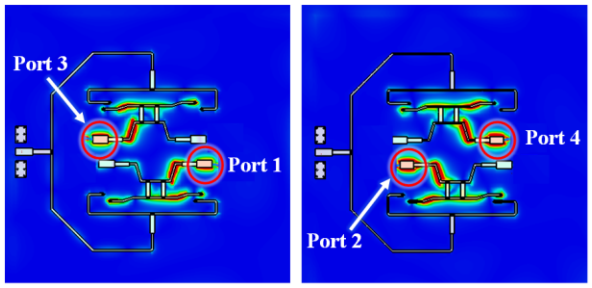

(a) (b)

Fig. 11. *E*-field distribution of the feeding network at 9.375 GHz. (a) Sequential feeding for RHCP. (b) Sequential feeding for LHCP.

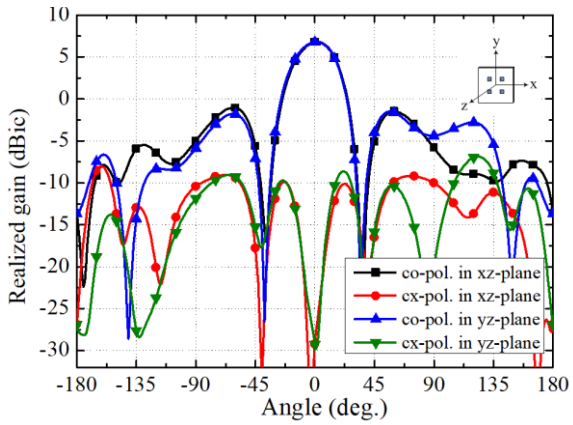

(a)

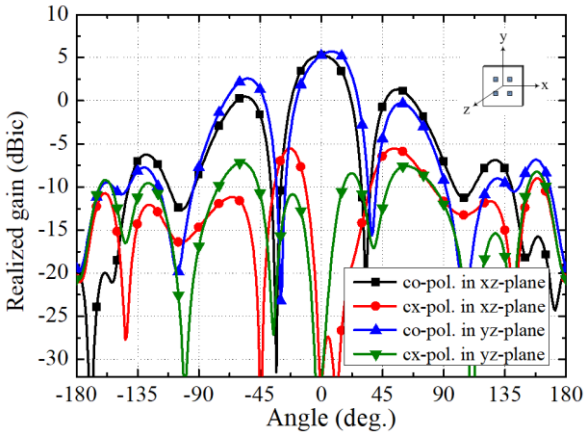

(b)

Fig. 12. The simulated radiation patterns at 9.375 GHz. (a) RHCP. (b) LHCP.

Fig. 11 shows the electric field distribution of the feeding network. When signals are excited to port 1 and port 3, port 2 and port 4 are isolated as shown Fig. 11(a). On the contrary, when signals are excited to port 2 and port 4, port 1 and port 3 are isolated like as Fig. 11(b).

Fig. 12(a) and Fig. 12(b) show the simulated radiation patterns of the dual-CP antenna in xz-plane and xy-plane at the design frequency of 9.375 GHz, respectively. The RHCP sum (Σ) gain is 6.7 dBic, and the LHCP sum (Σ) gain is 5.3 dBic. HPBW are 31.5° ~ 36° of sum (Σ) pattern in both azimuth and elevation planes, respectively.

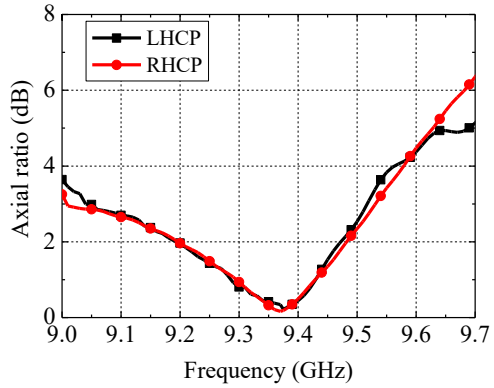

Fig. 13. The axial ratio of the dual-CP antenna.

Fig. 13 shows the axial ratio of the dual-CP antenna with the simulation results. The simulated 3 dB bandwidth of the axial ratio of RHCP and LHCP are 160 MHz (9.29 GHz ~ 9.45 GHz) and 160 MHz (9.29 GHz ~ 9.45 GHz).

When port 2 and port 4 with 180° phase delay are simultaneously fed, the four microstrip patch antennas have sequential feeding (C-point 0°, D-point 90°, A-point 180°, B-point 270°) in the opposite direction and generate the LHCP sum (Σ) pattern. When signals are excited to port 2 and port 4, port 1 and port 3 are isolated. Therefore, the proposed dual-CP antenna can receive both RHCP and LHCP, and the analyzed antenna characteristics confirmed that it is suitable for target detection and monopulse radar applications.

In the future, the proposed dual-CP antenna will be added with feeding circuit with 180° phase difference, and performance test will be carried out.

V. Conclusion

A compact and planar target detection antenna for receiving radar signals is proposed in this letter, which consists of 2 x 2 microstrip patch antenna array and a symmetric feeding line. The designed antenna has only two ports without rat-race couplers and a simple comparator circuit comparing with reference antennas. It has circular polarization (RHCP or LHCP) with the sequence feeding in 9.375 GHz (X-band) and difference (Δ) pattern with new simultaneous feeding in all polarizations. The measured results show that the designed antenna has achieved a good null depth of over 34.5 dB in all direction, a peak sum gain 4.51 dB at 9.375 GHz and a 3-dB axial ratio (AR) bandwidth is 160 MHz. Since both patterns (Σ, Δ) are formed at the same time and equal radiation level in all polarizations, the designed antenna is suitable for receiving radar signals and target detection applications. The feeding network which can receive both RHCP and LHCP is also proposed, and the simulation results confirm that the dual-CP antenna is applicable to monopulse applications.

References

[1] S. M. Sherman, *Monopulse Principles and Techniques.* Dedham, MA: Artech House, 1984.

[2] H. Gharibi, and F. H. Kashani, "Design of a wideband monopulse antenna using four conical helix antennas," *Prog. Electromagnetics Research Lett*., vol. 29, pp.25–33, Jan. 2012.

[3] K. S. Ang, Y. C. Leong, and C. H. Lee, "A wide-band monopulse comparator with complete nulling in all delta channels throughout sum channel bandwidth," *IEEE Trans. Microw. Theory and Tech.,* vol. 51, pp.371–373, Feb. 2003.

[4] H. Wang, D. -G. Fang, and X. G. Chen, "A compact single layer monopulse microstrip antenna array," *IEEE Trans. Antennas Propargat.,* vol. 54, no. 2, pp.503–509, Feb. 2006.

[5] J. Aliasgari, and Z. Atlasbaf, "A novel compact monopulse parallel-plate slot array antenna," *IEEE Antenna Wirel. Proapg. Lett,* vol. 15, pp.762–765, Mar. 2016.

[6] N. Yang, C. Caloz, and K. Wu, "Monopulse comparator with frequency-independent delta-channel nulls for high-resolution tracking radar," *Electron. Lett.,* vol. 47, no. 5, pp.339–340, Mar. 2011.

[7] H. Gharibi, and F. Hodjatkashani, "Design of a compact high-efficiency circularly polarized monopulse cavity-backed substrate integrated waveguide antenna," *IEEE Trans. Antennas Propargat.,* vol. 63, no. 9, pp.4250–4256, Sep. 2015.

[8] H. Chu, J. –X. Chen, S. Luo, and Y. -X Guo, "A Millimeter-wave filtering onopulse antenna array based on substrate integrated waveguide technology," *IEEE Trans. Antennas Propagat.,* vol. 64, no. 1, pp.316–321, Jan. 2016.

[9] H. Gharibi, and F. H. Kashani, "Design of compact circularly polarized dual-mod monopulse cavity-backed substrate integrated waveguide antenna," *IEEE Antennas Wireless. Propargt. Lett.,* vol. 14, pp.519–522. Nov. 2015.

[10] B. Liu et al., "Substrate integrated waveguide (SIW) monopulse slot antenna array," *IEEE Trans. Propagat.,* vol. 57, no. 1, pp. 275-279, Jan. 2009.

[11] F. Yu, Y. Xie, and L. Zhang, "Single patch antenna with monopulse patterns," *IEEE Micro. Wirel. Compon. Lett.,* vol. 26, no. 10, pp.762–764. Oct. 2016.

[12] T. P. Cencich, J. C. McDonnell, and T. W. Samson, "Radiation modes of an outside fed 4-arm conical spiral," *Proc. Int. ACES Symp*., Denver, 2018, pp. 1–2.

[13] E. Mehboodi, M. Movahhedi, and A. Heidari, "Wideband dual-polarised SAW spiral antenna for monopulse system," *IET Microw. Antennas Propagat.,* vol. 12, no. 4, pp.607–611, Mar. 2018.